

Analytic Mode Normalization for the Kerr Nonlinearity Parameter: Prediction of Nonlinear Gain for Leaky Modes

I. Allayarov,^{1,*} S. Upendar,¹ M. A. Schmidt,^{2,3} and T. Weiss¹

¹*4th Physics Institute and Research Center SCoPE, University of Stuttgart, Pfaffenwaldring 57, D-70550 Stuttgart, Germany*

²*Leibniz Institute of Photonic Technology, Albert-Einstein-Strasse 9, D-07745 Jena, Germany*

³*Otto Schott Institute of Material Research, Friedrich Schiller University of Jena, Fraunhoferstrasse 6, D-07743 Jena, Germany*

 (Received 11 July 2018; published 21 November 2018)

Based on the resonant-state expansion with analytic mode normalization, we derive a general master equation for the nonlinear pulse propagation in waveguide geometries that is valid for bound and leaky modes. In the single-mode approximation, this equation transforms into the well-known nonlinear Schrödinger equation with a closed expression for the Kerr nonlinearity parameter. The expression for the Kerr nonlinearity parameter can be calculated on the minimal spatial domain that spans only across the regions of spatial inhomogeneities. It agrees with previous vectorial formulations for bound modes, while for leaky modes the Kerr nonlinearity parameter turns out to be a complex number with the imaginary part providing either nonlinear loss or even gain for the overall attenuating pulses. This nonlinear gain results in more intense pulse compression and stronger spectral broadening, which is demonstrated here on the example of liquid-filled capillary-type fibers.

DOI: 10.1103/PhysRevLett.121.213905

Optical pulses can be significantly influenced by the nonlinear response of a medium, including self-focusing, self-phase modulation, four-wave mixing, and Raman scattering [1], all mediated by the optical Kerr effect. These effects are used in optical fibers for extreme spectral broadening referred to as supercontinuum generation [1,2], having a large number of applications [3–8]. Owing to their tuning capabilities, many of these applications involve capillaries or hollow-core fibers filled with gas or liquid [5,6,8–11]. However, these waveguides are typically governed by leaky modes that lack—in contrast to their guided counterparts—a rigorous theoretical description of nonlinear pulse propagation, which is mainly due to the increasing field amplitude in the most outer cladding.

For instance, the nonlinear Schrödinger equation [1] is characterized by the Kerr nonlinearity parameter γ , which includes the effective mode area and the material nonlinearity [12] and is calculated by perturbative [1,13–15] or iterative [16,17] approaches. While iterative methods purely rely on numerical calculations, perturbative approaches require a well-defined mode normalization. For bound modes [example in Fig. 1(a)], the normalization can be defined as an integral of the absolute square value of the electric fields [1] or the axial component of the time-averaged Poynting vector [18,19] over the entire cross section of the fiber. In the case of leaky modes [example in Fig. 1(b)], the corresponding fields grow transverse to the direction of propagation with distance to the waveguide or fiber. Hence, typical expressions used for the modal normalization diverge, resulting in an unphysically vanishing Kerr nonlinearity parameter. Several approaches

have been suggested to bypass this issue, such as using a restricted area of normalization defined by radiation caustic [20] and applying a complex coordinate transformation to regions outside the spatial inhomogeneities [19] for suppressing the divergence (equivalent to perfectly matched layers [21]). However, these approaches are prone to failure, since they include certain parameters that need to be adapted to a specific geometry. In contrast, analytic normalization schemes, which are commonly used for three-dimensional optical resonators [22–25], can be readily applied to any geometry with a homogeneous surrounding. An analytic expression for the mode normalization in waveguide geometries can be found for slab waveguides in Ref. [26] and for optical fibers in Ref. [27].

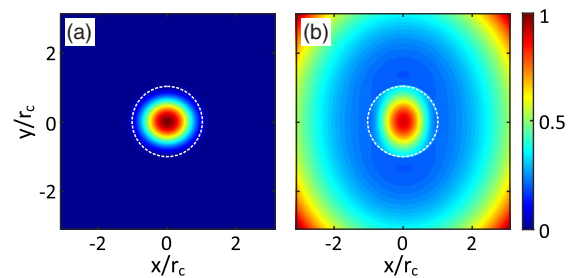


FIG. 1. Spatial distribution of the z component of the real-valued Poynting vector of fundamental fiber modes ($\lambda_0 = 800$ nm) for two geometries (core radius $r_c = 0.3$ μm). (a) Guided mode in a cylindrical step-index fiber with bismuth oxide (Bi_2O_3 , $n = 2.05$) core and air cladding and (b) leaky mode in a Bi_2O_3 capillary filled with carbon disulfide (CS_2 , $n = 1.6$).

Based on the correct mode normalization, it is possible to set up the so-called resonant-state expansion [22–28], which is a rigorous perturbative method that uses the normalized resonant states of a reference system for describing the optical properties of a perturbed system.

In this Letter, we use the resonant-state expansion with the analytic mode normalization to derive a master equation for the nonlinear pulse propagation that allows for a rigorous description of both bound and leaky modes in waveguide geometries. This equation is fully vectorial and includes possible Raman scattering, intermodal cross talk, and backscattering. If the latter three effects can be neglected, the master equation reduces to the standard nonlinear Schrödinger equation with a redefined Kerr nonlinearity parameter γ that can be calculated straightforwardly with any linear Maxwell solver on a small computational domain that includes all spatial inhomogeneities. For leaky modes, γ turns out to be a complex number, confirming previous studies based on analytical calculations [15] as well as iterative approaches [16,17]. We find that its imaginary part can lead to nonlinear gain in addition to linear loss, resulting in pulse compression and spectral broadening, as demonstrated here for capillary fibers.

In waveguide geometries, the permittivity and the permeability tensors ϵ and μ , respectively, possess a translational symmetry along one spatial direction, which we choose to be the z direction. Hence, we may use the Fourier transformation

$$\hat{f}(\mathbf{r}_{\parallel}, \beta) = \frac{1}{2\pi} \int_{-\infty}^{+\infty} f(\mathbf{r}_{\parallel}, z) e^{-i\beta z} dz, \quad (1)$$

where \mathbf{r}_{\parallel} denotes the spatial coordinates in the xy plane and the hat implies Fourier space. Thus, the frequency-domain representation of Maxwell's equations [time dependence $\exp(-i\omega t)$] can be written (in Gaussian units [29]) as [28]

$$\hat{\mathbb{M}}(\mathbf{r}_{\parallel}, \beta) \hat{\mathbb{F}}(\mathbf{r}_{\parallel}) = \hat{\mathbb{J}}(\mathbf{r}_{\parallel}), \quad (2)$$

with the matrix and vector operators

$$\hat{\mathbb{M}}(\mathbf{r}_{\parallel}, \beta) = \begin{pmatrix} \epsilon k_0 & -\hat{\nabla}_{\beta} \times \\ -\hat{\nabla}_{\beta} \times & \mu k_0 \end{pmatrix} \quad \text{and} \quad \hat{\nabla}_{\beta} \equiv \begin{pmatrix} \partial_x \\ \partial_y \\ i\beta \end{pmatrix} \quad (3)$$

and the field and current vectors

$$\hat{\mathbb{F}}(\mathbf{r}_{\parallel}) = \begin{pmatrix} \hat{\mathbf{E}} \\ i\hat{\mathbf{H}} \end{pmatrix} \quad \text{and} \quad \hat{\mathbb{J}}(\mathbf{r}_{\parallel}) = \begin{pmatrix} \hat{\mathbf{J}} \\ 0 \end{pmatrix}, \quad (4)$$

respectively, where $k_0 = \omega/c$ is the wave number and $\hat{\mathbf{J}} = -4\pi i \hat{\mathbf{j}}/c - 4\pi k_0 \hat{\mathbf{P}}_{\text{NL}}$ is the source of the fields.

Solutions of Eq. (2) with general source $\hat{\mathbb{J}}(\mathbf{r}_{\parallel})$ can be obtained from the Green's dyadic (GD) $\hat{\mathbb{G}}_{\beta}(\mathbf{r}_{\parallel}, \mathbf{r}'_{\parallel})$ with the constitutive equation

$$\hat{\mathbb{M}}(\mathbf{r}_{\parallel}, \beta) \hat{\mathbb{G}}_{\beta}(\mathbf{r}_{\parallel}, \mathbf{r}'_{\parallel}) = \hat{\mathbb{I}} \delta(\mathbf{r}_{\parallel} - \mathbf{r}'_{\parallel}), \quad (5)$$

where $\hat{\mathbb{I}}$ is the 6×6 identity matrix.

The GD can be decomposed in basis functions, namely, the resonant states (RSs) [22]. The RSs are a discrete set of solutions of the homogeneous Maxwell equations with outgoing boundary conditions at wave numbers β_m :

$$\hat{\mathbb{M}}(\mathbf{r}_{\parallel}, \beta_m) \hat{\mathbb{F}}_m(\mathbf{r}_{\parallel}) = 0. \quad (6)$$

Note that due to reciprocity, for each eigenvector $\hat{\mathbb{F}}_m$ with eigenvalue β_m , there is another, “reciprocal conjugate” eigensolution denoted by $\hat{\mathbb{F}}_m^R$ at $-\beta_m$. The eigenvalues β_m correspond to poles of the GD. Thus, according to the Mittag-Leffler theorem and the reciprocity principle, the GD can be expanded as follows [27]:

$$\hat{\mathbb{G}}_{\beta}(\mathbf{r}_{\parallel}, \mathbf{r}'_{\parallel}) = -\sum_m \frac{\hat{\mathbb{F}}_m(\mathbf{r}_{\parallel}) \otimes \hat{\mathbb{F}}_m^R(\mathbf{r}'_{\parallel})}{2N_m(\beta - \beta_m)} + \hat{\mathbb{G}}_{\beta}^{\text{cut}}. \quad (7)$$

Here, we have introduced the normalization constant N_m that provides the correct weight to the RSs, since the eigenvectors $\hat{\mathbb{F}}_m$ are defined by Eq. (6) only up to a constant factor. The term $\hat{\mathbb{G}}_{\beta}^{\text{cut}}$ denotes possible cut contributions due to the analytic continuation on the complex β plane [23,26,27], which can be replaced by cut poles in numerical calculations [23,26].

As shown in Ref. [27], the analytic expression for the normalization constant of the RSs in fiber geometries is

$$N_m = S_m + L_m, \quad (8)$$

with the surface term

$$S_m = \int_0^{2\pi} \int_0^{r_n} \rho (\hat{E}_{m,\rho} \hat{H}_{m,\phi} - \hat{E}_{m,\phi} \hat{H}_{m,\rho}) d\rho d\phi, \quad (9)$$

where r_n is the normalization radius, and the line term

$$L_m = \frac{\epsilon \mu k_0^2 + \beta_m^2}{2(\epsilon \mu k_0^2 - \beta_m^2)^2} \int_0^{2\pi} \left(\hat{E}_{m,z} \frac{\partial \hat{H}_{m,z}}{\partial \phi} - \hat{H}_{m,z} \frac{\partial \hat{E}_{m,z}}{\partial \phi} \right)_{\rho=r_n} d\phi + \frac{k_0 \beta_m r_n^2}{2(\epsilon \mu k_0^2 - \beta_m^2)^2} \int_0^{2\pi} \left\{ \mu \left[\left(\frac{\partial \hat{H}_{m,z}}{\partial \rho} \right)^2 - \rho \hat{H}_{m,z} \frac{\partial}{\partial \rho} \left(\frac{1}{\rho} \frac{\partial \hat{H}_{m,z}}{\partial \rho} \right) \right] + \epsilon \left[\left(\frac{\partial \hat{E}_{m,z}}{\partial \rho} \right)^2 - \rho \hat{E}_{m,z} \frac{\partial}{\partial \rho} \left(\frac{1}{\rho} \frac{\partial \hat{E}_{m,z}}{\partial \rho} \right) \right] \right\}_{\rho=r_n} d\phi. \quad (10)$$

Based on the GD in Eq. (7), the fields generated by a source $\hat{\mathbb{J}}$ can be calculated as

$$\begin{aligned}\hat{\mathbb{F}}(\mathbf{r}_{\parallel}, \beta; \omega) &= \int \hat{\mathbb{G}}_{\beta}(\mathbf{r}_{\parallel}, \mathbf{r}'_{\parallel}; \omega) \hat{\mathbb{J}}(\mathbf{r}'_{\parallel}, \beta; \omega) d\mathbf{r}'_{\parallel} \\ &= -\sum_m \frac{\hat{\mathbb{F}}_m(\mathbf{r}_{\parallel}; \omega)}{2N_m(\beta - \beta_m)} \int \hat{\mathbb{F}}_m^R(\mathbf{r}'_{\parallel}; \omega) \cdot \hat{\mathbb{J}}(\mathbf{r}'_{\parallel}, \beta; \omega) d\mathbf{r}'_{\parallel}.\end{aligned}\quad (11)$$

Next, we decompose the field on the left-hand side as

$$\hat{\mathbb{F}}(\mathbf{r}_{\parallel}, \beta; \omega) = \sum_m a_m(\beta, \omega) \frac{1}{\sqrt{N_m}} \hat{\mathbb{F}}_m(\mathbf{r}_{\parallel}; \omega), \quad (12)$$

with a_m as the modal amplitude. Substituting $\hat{\mathbb{F}}$ in Eq. (11) by Eq. (12), evaluating the result for each $\hat{\mathbb{F}}_m$ independently, and carrying out the inverse Fourier transform of Eq. (1), we obtain

$$(\partial_z - i\beta_m) a_m(z; \omega) = \frac{1}{2i\sqrt{N_m}} \int \hat{\mathbb{F}}_m^R(\mathbf{r}_{\parallel}; \omega) \cdot \mathbb{J}(\mathbf{r}_{\parallel}, z; \omega) d\mathbf{r}_{\parallel}.\quad (13)$$

Finally, we consider \mathbb{J} to be the nonlinear polarization, which yields after the transformation from the frequency to the time domain the general master equation for the nonlinear pulse propagation:

$$\begin{aligned}\partial_z a_m(z; t) &= i\beta_m(t) * a_m(z; t) \\ &\quad - \frac{2\pi}{c} \partial_t \int \mathbf{e}_m^R(\mathbf{r}_{\parallel}; t) * \mathbf{P}_{\text{NL}}(\mathbf{r}; t) d\mathbf{r}_{\parallel}.\end{aligned}\quad (14)$$

Here, $*$ denotes convolutions in the time domain, and $\mathbf{e}_m^R(\mathbf{r}_{\parallel}; t) \equiv \mathbf{E}_m^R(\mathbf{r}_{\parallel}; t) / \sqrt{N_m}$ is the normalized electric field in the time domain. This equation is fully vectorial and contains no approximation so far. The only limitation of Eq. (14) is that the expansion of the GD in terms of RSs is not straightforward in the external regions outside the spatial inhomogeneities [24,25]. Thus, the nonlinear polarization should be restricted to the region of spatial inhomogeneities, i.e., excluding the homogeneous exterior. Note that \mathbf{P}_{NL} contains implicitly the modal expansion Eq. (12), so that Eq. (14) constitutes a rigorous description of any nonlinear effect in terms of the RSs, including both bound and leaky modes. In the following, we derive exemplarily the nonlinear Schrödinger equation.

For most materials, the dominating nonlinear contribution in \mathbf{P}_{NL} is the third-order nonlinear susceptibility [1]. In general, this is a convolution in time of the $\chi^{(3)}$ tensor with the electric field. Assuming an instantaneous nonlinear response, we obtain

$$\mathbf{P}_{\text{NL}}(\mathbf{r}; t) \approx \chi^{(3)} \mathbb{E}(\mathbf{r}; t) \mathbf{E}(\mathbf{r}; t) \mathbf{E}(\mathbf{r}; t), \quad (15)$$

where \mathbb{E} denotes tensorial multiplication. For the electric fields in Eq. (15), we use the Fourier transform of Eq. (12) from the frequency to the time domain. Considering pulses that are centered around a frequency ω_0 with a finite spectral width and assuming that $\hat{\mathbf{e}}_m$ depends only weakly on the frequency around ω_0 , the fields can be written as

$$\mathbf{E}(\mathbf{r}; t) = \sum_m a_m(z; t) \mathcal{E}_m(\mathbf{r}_{\parallel}) + \text{c.c.} \equiv \mathcal{E}(\mathbf{r}; t) e^{-i\omega_0 t} + \text{c.c.}, \quad (16)$$

where $\mathcal{E}_m(\mathbf{r}_{\parallel}) \equiv \hat{\mathbf{e}}_m(\mathbf{r}_{\parallel}; \omega_0)$ and $\mathcal{E}(\mathbf{r}; t)$ is the envelope for the dominant plane wave with frequency ω_0 . Thus, we obtain dominant contributions of \mathbf{P}_{NL} in Eq. (15) oscillating with ω_0 and $3\omega_0$. For isotropic materials and by taking into account the permutation symmetry of the $\chi^{(3)}$ tensor, the resulting nonlinear polarization yields [14]

$$\mathbf{P}_{\text{NL}} \approx \frac{\chi_i^{(3)}}{4} [2(\mathcal{E} \cdot \mathcal{E}^*) \mathcal{E} + (\mathcal{E} \cdot \mathcal{E}) \mathcal{E}^*] e^{-i\omega_0 t}, \quad (17)$$

where $\chi_i^{(3)} \equiv \chi_{xxxx}^{(3)}$. Thus, the propagation equation becomes

$$\partial_z a_m \approx i\beta_m * a_m + \sum_{n,p,q} i \frac{2\pi}{c} \partial_t \alpha_{m,n,p,q} a_n a_p^* a_q, \quad (18)$$

with

$$\begin{aligned}\alpha_{m,n,p,q} &= \int \frac{\chi_i^{(3)}}{4} [2(\mathcal{E}_m^R \cdot \mathcal{E}_q)(\mathcal{E}_n \cdot \mathcal{E}_p^*) \\ &\quad + (\mathcal{E}_m^R \cdot \mathcal{E}_p^*)(\mathcal{E}_n \cdot \mathcal{E}_q)] d\mathbf{r}_{\parallel}.\end{aligned}\quad (19)$$

In the single-mode approximation, Eq. (18) transforms into the standard nonlinear Schrödinger equation. First, we separate β_m into real and imaginary parts $\bar{\beta}_m$ and $\bar{\alpha}_m$, respectively. Expanding them into Taylor series around ω_0 yields

$$\bar{\beta}_m \approx \bar{\beta}_m^{(0)} + \bar{\beta}_m^{(1)}(\omega - \omega_0) + \frac{\bar{\beta}_m^{(2)}}{2}(\omega - \omega_0)^2, \quad (20)$$

where $\bar{\beta}_m^{(n)} = \partial^n \bar{\beta}_m / \partial \omega^n|_{\omega_0}$, and $\bar{\alpha}_m(\omega) \approx \bar{\alpha}_m(\omega_0) \equiv \bar{\alpha}_m^{(0)}$ when assuming a constant modal loss. By introducing

$$a_m(z; t) \equiv A_m(z; t) e^{-i\omega_0 t + i\bar{\beta}_m^{(0)} z}, \quad (21)$$

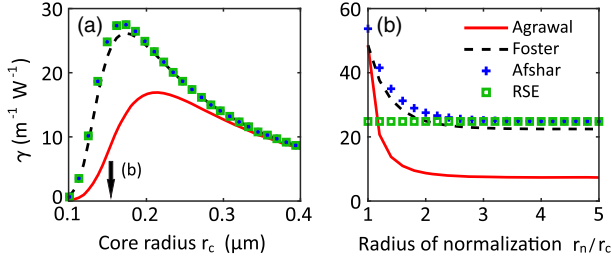


FIG. 2. Comparison of different approaches for calculating the Kerr nonlinearity parameter γ of the fundamental bound mode of a Bi_2O_3 fiber located in air ($\lambda_0 = 800 \text{ nm}$): (a) γ as a function of core radius r_c for a radius of normalization $r_n = 5r_c$ and (b) dependence of γ on r_n for $r_c = 0.15 \mu\text{m}$ [arrow in (a)].

we obtain the well-known nonlinear Schrödinger equation

$$\partial_z A_m \approx i\gamma \left(1 - \frac{1}{i\omega_0} \partial_\tau\right) |A_m|^2 A_m - i \frac{\bar{\beta}_m^{(2)}}{2} \partial_\tau^2 A_m - \bar{\alpha}_m^{(0)} A_m, \quad (22)$$

with $\gamma = 2\pi k_0 \alpha_{m,m,m,m}$ as the Kerr nonlinearity parameter and $\tau = t - \bar{\beta}_m^{(1)} z$ as the retarded time. It has to be emphasized that Eq. (22) is obtained in a rigorous way without any slowly varying approximation. Moreover, it can be readily applied to both bound and leaky modes due to the analytic mode normalization. For leaky modes, the correctly normalized fields and, thus, γ are complex quantities, in agreement with previous findings [15–17]. Particularly, our γ equals that of Ref. [15] when replacing their normalization by the analytic expression, which ensures a straightforward implementation in numerical calculations [27].

Let us now compare our approach for the calculation of γ with other perturbative formulations for bound modes. Since bound modes exhibit a real propagation constant, reciprocal conjugation can be replaced by the usual complex conjugation, i.e., $\mathcal{E}_m^R = \mathcal{E}_m^*$. Hence, one can show that our γ has exactly the same form as in the vectorial approach described in Refs. [12,14,15], whereas the scalar approaches of Refs. [1,13] are approximatively valid for vanishing longitudinal electromagnetic field components. Figure 2(a) displays γ as a function of core radius r_c for the step-index fiber considered in Ref. [14] with Bi_2O_3 core ($\chi_{\text{Bi}_2\text{O}_3}^{(3)} = 3.4 \times 10^{-13} \text{cm}^2 \text{statV}^{-2}$) surrounded by air. The results have been obtained by the weakly guiding approximation [1] (Agrawal, red line), its slightly improved version suggested in Ref. [13] (Foster, black dashed line), the fully vectorial approach [14] (Afshar, blue crosses), and our approach based on the resonant-state expansion (RSE, green square dots). It can be seen that our approach provides exactly the same results as the fully vectorial one. In contrast, both scalar approaches (Agrawal and Foster) deviate significantly for small core radii, which can be explained by the large longitudinal field components [14]. The advantage of our approach compared to the fully vectorial one is that, in

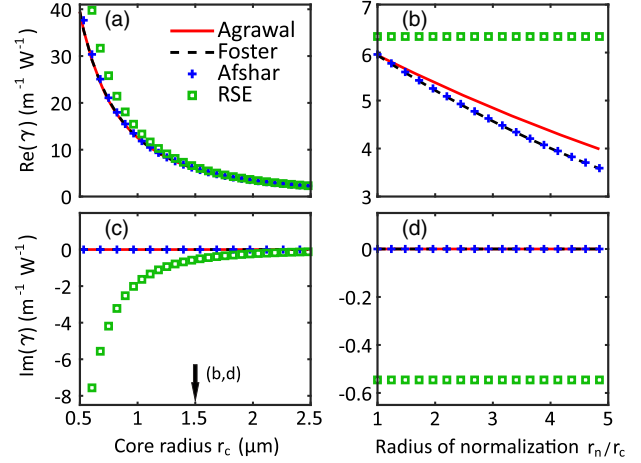


FIG. 3. Comparison of different approaches for calculating γ of the fundamental leaky mode of a Bi_2O_3 capillary filled with CS_2 ($\lambda_0 = 800 \text{ nm}$). The top and bottom panels depict the real and imaginary parts, respectively, of γ as functions of core radius r_c [(a) and (c) with $r_n = r_c$] and radius of normalization r_n [(b) and (d) with $r_c = 1.5 \mu\text{m}$; see the arrow in (c)], respectively.

numerical calculations, we can restrict the area of normalization to the regions of spatial inhomogeneities, which is in the present case the fiber core. This can be seen in Fig. 2(b), where γ is displayed as a function of the radius of normalization r_n for a fixed core radius of $r_c = 1.5 \mu\text{m}$. While previous approaches [1,13,14] require some finite radius r_n of roughly $3r_c$ in order to exhibit a deviation of less than 5% to their exact value of normalization for $r_n \rightarrow \infty$, our approach is independent of the radius of normalization for all $r_n \geq r_c$, as expected from Eq. (8). This fact makes numerical calculations more efficient, especially for complex fiber geometries such as photonic crystal fibers [30] and situations with extended evanescent fields.

As a rather simple example for leaky modes, we consider a Bi_2O_3 capillary fiber that has similar dimensions as the experimentally fabricated Bi_2O_3 fibers in Refs. [31,32]. In our case, the capillary is filled with CS_2 [6,33], which we assume here to be the only nonlinear material, since $\chi_{\text{CS}_2}^{(3)} = 1.8 \times 10^{-12} \text{cm}^2 \text{statV}^{-2} \gg \chi_{\text{Bi}_2\text{O}_3}^{(3)}$. Figures 3(a) and 3(c) show real and imaginary parts of γ as functions of the core radius r_c . For the scalar and the fully vectorial approaches, we have used $r_n = r_c$ as an optimum radius of normalization for each core radius, which corresponds to the minimum deviation to our approach [Fig. 3(b)]. In the strong guidance or subwavelength regime ($2r_c < \lambda_0$), these approaches begin to deviate from our value for the real part of γ [Fig. 3(a)]. For large core radii ($2r_c \gg \lambda_0$), the deviation between the different approaches becomes smaller.

In contrast to bound modes, γ has a nonvanishing imaginary part for leaky modes [Fig. 3(c)]. While this is expected from previous works [15–17], we find that, depending on the fiber parameters, $\text{Im}(\gamma)$ can change its

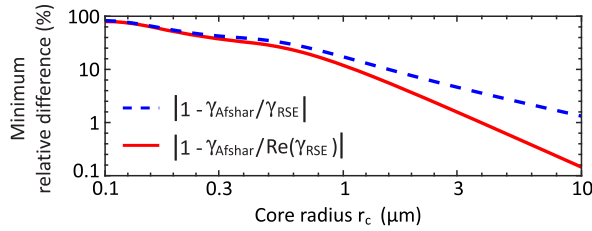


FIG. 4. Minimum relative differences between the vectorial γ_{Afshar} and our γ_{RSE} (blue dashed line) as well as $\text{Re}(\gamma_{\text{RSE}})$ (red solid line) as a function of the core radius for the Bi_2O_3 capillary filled with CS_2 ($\lambda_0 = 800$ nm).

sign, with $\text{Im}(\gamma) > 0$ as nonlinear loss and $\text{Im}(\gamma) < 0$ as nonlinear gain, which is not a contradiction to previous works [29]. The mechanism of the nonlinear gain can be explained by a self-focusing that reduces the pulse intensity at the core-cladding interface, which in turn decreases the energy dissipation through the cladding.

Let us now consider γ as a function of the normalization radius r_n [Figs. 3(b) and 3(d)] for a fixed core radius of $r_c = 1.5$ μm . While our approach yields the same γ for all radii of normalization, the other approaches result in $\gamma \rightarrow 0$ for $r_n \rightarrow \infty$. The minimum deviation of the real part of γ (red solid line) and its absolute value (blue dashed line) between the approach by Afshar and our approach is displayed in Fig. 4 as a function of core radius r_c . Evidently, the imaginary part of γ is the main reason for the significant deviation for larger core radii.

Next, we study the influence of the imaginary part of γ on the pulse propagation. For our numerical simulations, we consider the Bi_2O_3 capillary fiber with a radius of $r_c = 10$ μm filled with CS_2 (results for other core radii are given in Ref. [29]). The numerical solution of Eq. (22) is calculated by the split-step Fourier method [1,4,34]. Figures 5(c) and 5(d) display the spectral and temporal evolution, respectively, of the initial pulse with $\gamma_{\text{Afshar}} = 141.5$ $\text{km}^{-1} \text{W}^{-1}$ obtained from the fully vectorial approach. The results in Figs. 5(a) and 5(b) have been obtained for $\gamma_{\text{RSE}} = (141.7 - 1.9i)$ $\text{km}^{-1} \text{W}^{-1}$ based on our approach. In the latter case [Fig. 5(a)], we can clearly see an increasing spectral broadening compared to the fully vectorial approach [Fig. 5(c)] that is accompanied by a narrowing in the corresponding temporal evolutions [Figs. 5(b) and 5(d)]. We conclude that the negative imaginary part of the Kerr nonlinearity parameter leads to pulse compression, which in turn gives rise to spectral broadening.

In conclusion, we present here a new and general approach for simulating nonlinear pulse propagation in waveguides and optical fibers based on the resonant-state expansion with analytic mode normalization. This rigorous approach does not require any slowly varying amplitude approximation and can be readily applied to both bound and leaky modes, with the analytic form of the normalization allowing for a restriction of the computational

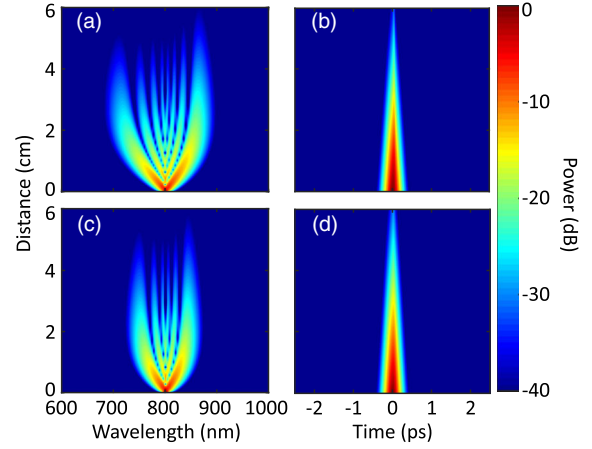


FIG. 5. Numerical simulation showing the nonlinear pulse propagation inside a CS_2 -filled Bi_2O_3 capillary ($r_c = 10$ μm) with $\gamma_{\text{RSE}} = (141.7 - 1.9i)$ $\text{km}^{-1} \text{W}^{-1}$ [(a),(b)] and $\gamma_{\text{Afshar}} = 141.5$ $\text{km}^{-1} \text{W}^{-1}$ [(c),(d)]. The input hyperbolic secant shape pulse at 800 nm has 15 kW peak power and 140 fs FWHM. Calculated dispersion parameters of the fiber are $\bar{\beta}^{(2)} = -0.82$ $\text{ps}^2 \text{km}^{-1}$, $\bar{\beta}^{(3)} = 1.05 \times 10^{-3}$ $\text{ps}^3 \text{km}^{-1}$, and $\bar{\beta}^{(4)} = -1.78 \times 10^{-6}$ $\text{ps}^4 \text{km}^{-1}$, with an attenuation coefficient of $\bar{\alpha}^{(0)} = 60.15$ m^{-1} .

domain to regions of spatial inhomogeneities. Most importantly, we find that, in the case of leaky modes, the Kerr nonlinearity parameter has an imaginary part that provides either nonlinear loss or nonlinear gain for overall attenuating pulses that can significantly influence the spectral and temporal evolution of an ultrashort pulse. While our example of a capillary fiber is rather simple, leaky modes play a crucial role in a large number of fiber geometries [5,8–11]. For all these geometries, our theory opens new routes for tailoring the nonlinear pulse propagation in optical fibers with application in fields such as supercontinuum generation and pulse compression.

We acknowledge support from DFG SPP 1839 and the MWK Baden-Württemberg.

*i.allayarov@pi4.uni-stuttgart.de

- [1] G. Agrawal, *Nonlinear Fiber Optics* (Academic, New York, 2013).
- [2] A. Zheltikov, *Supercontinuum Generation* (Springer, New York, 2003).
- [3] M. Nisoli, *Appl. Phys. Lett.* **68**, 2793 (1996).
- [4] J. M. Dudley, G. Genty, and S. Coen, *Rev. Mod. Phys.* **78**, 1135 (2006).
- [5] P. S. J. Russell, P. Hölzer, W. Chang, A. Abdolvand, and J. Travers, *Nat. Photonics* **8**, 278 (2014).
- [6] S. Kedenburg, T. Gissibl, T. Steinle, A. Steinmann, and H. Giessen, *Opt. Express* **23**, 8281 (2015).
- [7] M. Chemnitz, M. Gebhardt, C. Gaida, F. Stutzki, J. Kobelke, J. Limpert, A. Tünnermann, and M. A. Schmidt, *Nat. Commun.* **8**, 42 (2017).

- [8] R. Sollapur, D. Kartashov, M. Zürich, A. Hoffmann, T. Grigorova, G. Sauer, A. Hartung, A. Schwuchow, J. Bierlich, J. Kobelke *et al.*, *Light Sci. Appl.* **6**, e17124 (2017).
- [9] F. Tani, F. Köttig, D. Novoa, R. Keding, and P. S. J. Russell, *Photonics Res.* **6**, 84 (2018).
- [10] V. Pureur and J. M. Dudley, *Opt. Lett.* **35**, 2813 (2010).
- [11] O. Vanvincq, A. Kudlinski, A. Bétourné, Y. Quiquempois, and G. Bouwmans, *J. Opt. Soc. Am. B* **27**, 2328 (2010).
- [12] M. Chemnitz and M. A. Schmidt, *Opt. Express* **24**, 16191 (2016).
- [13] M. A. Foster, K. D. Moll, and A. L. Gaeta, *Opt. Express* **12**, 2880 (2004).
- [14] S. Afshar and T. M. Monro, *Opt. Express* **17**, 2298 (2009).
- [15] G. Li, C. M. de Sterke, and S. Palomba, *Opt. Lett.* **42**, 1329 (2017).
- [16] A. Maslov, *Opt. Lett.* **39**, 4396 (2014).
- [17] M. M. Elsayy and G. Renversez, *Opt. Lett.* **43**, 2446 (2018).
- [18] R. Sammut and A. Snyder, *Appl. Opt.* **15**, 477 (1976).
- [19] R. Sammut and A. Snyder, *Appl. Opt.* **15**, 1040 (1976).
- [20] A. Snyder and J. Love, *Optical Waveguide Theory* (Chapman and Hall, London, 1983).
- [21] C. Sauvan, J. P. Hugonin, I. S. Maksymov, and P. Lalanne, *Phys. Rev. Lett.* **110**, 237401 (2013).
- [22] E. Muljarov, W. Langbein, and R. Zimmermann, *Europhys. Lett.* **92**, 50010 (2011).
- [23] M. B. Doost, W. Langbein, and E. A. Muljarov, *Phys. Rev. A* **87**, 043827 (2013).
- [24] T. Weiss, M. Mesch, M. Schäferling, H. Giessen, W. Langbein, and E. A. Muljarov, *Phys. Rev. Lett.* **116**, 237401 (2016).
- [25] T. Weiss, M. Schäferling, H. Giessen, N. A. Gippius, S. G. Tikhodeev, W. Langbein, and E. A. Muljarov, *Phys. Rev. B* **96**, 045129 (2017).
- [26] S. V. Lobanov, G. Zorinians, W. Langbein, and E. A. Muljarov, *Phys. Rev. A* **95**, 053848 (2017).
- [27] S. Upendar, I. Allayarov, M. A. Schmidt, and T. Weiss, *Opt. Express* **26**, 22536 (2018).
- [28] E. Muljarov and T. Weiss, *Opt. Lett.* **43**, 1978 (2018).
- [29] See Supplemental Material at <http://link.aps.org/supplemental/10.1103/PhysRevLett.121.213905> for the dependence of the Kerr nonlinearity parameter on the core refractive index, the nonlinear pulse propagation in capillaries with small and large core radii, and the conversion to SI units.
- [30] P. S. J. Russell, *Science* **299**, 358 (2003).
- [31] K. Kikuchi and K. Taira, *Electron. Lett.* **38**, 166 (2002).
- [32] H. Ebendorff-Heidepriem, P. Petropoulos, S. Asimakis, V. Finazzi, R. C. Moore, K. Frampton, F. Koizumi, D. J. Richardson, and T. Monro, *Opt. Express* **12**, 5082 (2004).
- [33] M. Chemnitz, R. Scheibinger, C. Gaida, M. Gebhardt, F. Stutzki, S. Pompe, J. Kobelke, A. Tünnermann, J. Limpert, and M. A. Schmidt, *Optica* **5**, 695 (2018).
- [34] I. Cristiani, R. Tediosi, L. Tartara, and V. Degiorgio, *Opt. Express* **12**, 124 (2004).